Origins of the Fragmentation of Multipole Resonances Strengths in Light Open Shell Nuclei

N.G. Goncharova, N.D. Pronkina

Skobeltsyn Institute of Nuclear Physics, Moscow State University, 119992 Moscow, Russia

1. Particle-core coupling version of Shell Model.

Discovered in photoabsorption reactions, the giant resonances now are properly studied in electroexcitation of nuclei, where the multipolarity of excitation operators varied with growing momentum transfer and a large number of multipole resonances (MR) was revealed. The theoretical efforts in description of the magnitudes, energy distributions and partial characteristics of MR were only partly successful. Distribution and values of the multipole resonances (MR) strengths in open shell nuclei, especially in deformed ones, represent a challenge to the theory.

The main hindrance in theoretical investigation of MR in open shell nuclei is that the usual microscopical approach based on the conception of "particle-hole" doorway states is unfit for such nuclei.

One of the possible means to build a set of basic configurations which could be used as doorway states in the microscopic description of multipole resonances in open shell nuclei is to take into account the distribution of the "hole" among the states of residual (A-1) nuclei. The information on these distributions could be extracted from direct pick-up reaction spectroscopy.

In this paper would be shown some results of MR calculations based on the "particle-core coupling" version of shell model (PCC SM).

In PCC approach wave functions of excited nuclear states are expanded to a set of low-lying states of (A-1) nuclei coupled with a nucleon in a free orbit [1]:

$$\left|J_f,T_f\right\rangle = \sum_{(J'),j'} \alpha_f^{(J'),j'} \left|(J'E'T')_{A-1}\times(n'l'j'):J_f,T_f\right\rangle \qquad (1)$$

The basic configurations for MR in nuclei under investigation were built on those states of residual nuclei which have non vanishing spectroscopic factor $S=C^2N$ of pick-up reaction :

$$\left|J_i,T_i\right\rangle = \sum_{(J'),j} C_i^{(J'),j} \left|(J'E'T')_{A-1}\times(nlj):J_i,T_i\right\rangle \qquad (2)$$

Without violating the Pauli principle, PCC basis can be extended to include the configurations coupled to low-lying collective excitations of the target nucleus.

Matrix elements of operators in the space of (1,2) configurations could be represented as sums of m.e. one-particle transitions multiplied on spectroscopic amplitudes Z:

$$\left\langle J_fT_fM_T\left\|\hat{B}^J_{TM_T}\right\|J_iT_iM_T\right\rangle = \sum_{i,j_i,j_f} < j_f\left\|\hat{O}^J_{TM_T}\right\|j_i > \sqrt{2}\sqrt{2J_i+1}\cdot Z^J_{TM_T}(j_fj_i) \quad . \qquad (3)$$

The information on the structure of final and initial states of nucleus is embedded in spectroscopic amplitudes Z:

$$Z^{J}_{TM_T}(j_f j_i) = \sqrt{(2T+1)(2T_i+1)(2J_f+1)}\left\langle T_i M_T T 0 \middle| T_f M_T \right\rangle \times$$
$$\sum_{J'T'} C_i^{JT,j_i} \alpha_f^{J'T',j_f} (-1)^{J'-J_i+j_f-J} W(J_i J_f j_i j_f; JJ') (-1)^{T'-T_i+1/2-T} W(T_i T_f \tfrac{1}{2}\tfrac{1}{2}; TT'). \quad (4)$$

The matrix elements of PCC Hamiltonian involve the excitation energies of final nuclei levels:

$$\hat{H}_{ij} = (E' + \varepsilon_j + E_c)\delta_{ij} + \hat{V}_{ij}, \quad (5)$$

The estimation of magnitudes of residual interaction matrix elements was based as well on probabilities of pick-up reactions and corresponds to following scheme:

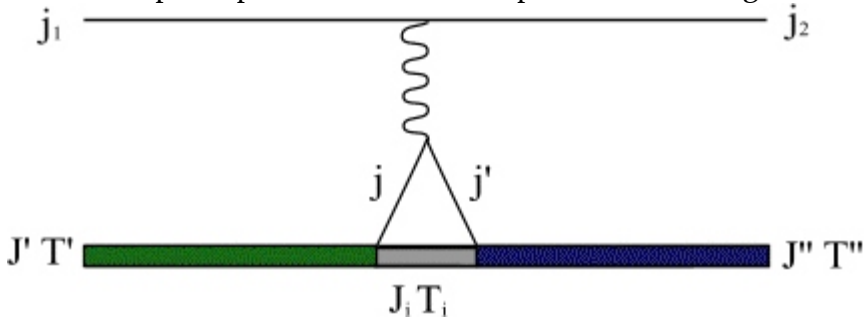

This paper represents PCC SM results for distributions of $1\hbar\omega$ isovector multipole resonances in photo- and electroexcitation cross section of sd-shell nuclei ^{22}Ne, ^{24}Mg ,^{26}Mg, ^{32}S, ^{34}S, ^{28}Si and ^{40}Ca. Some of these nuclei have considerable deformation in ground states. Their ground states deformations could not be measured directly. The parameters of deformation β for these even-even nuclei, estimated in [2], vary from 0.25 (^{34}S) up to 0.6 (^{24}Mg). In this work were used spectroscopic factors for sd-shell nuclei presented in [3].

This paper endeavors to show that connection between direct and resonance reactions could be used to get rather realistic microscopic description of MR' strength fragmentation.

2. Form factors of multipole $1\hbar\omega$ resonances.

Cross sections of electroexcitation contain information on nucleus structure in the form factors:

$$\frac{d^2\sigma(e,e')}{d\Omega d\omega} = \frac{4\pi\sigma_M}{\eta_R}\left\{\left(\frac{q_\mu^4}{q^4}\right)F_L^2(q,\omega) + \left(\frac{q_\mu^2}{2q^2} + tg^2\frac{\theta}{2}\right)F_T^2(q,\omega)\right\} \quad (7)$$

Transverse form factor is a sum of multipole form factors

$$F_T^2(q,\omega) = \sum_{J=1}^{J_{max}}\left\{F_{EJ}^2(q,\omega) + F_{MJ}^2(q,\omega)\right\}$$

The form factors of multipole resonances (MR) in nuclear electroexcitation cross section are functions of momentum q transferred to nucleus and for the transverse part is determined by the interplay of orbital and spin components of nucleon current:

$$\hat{T}^{el}_{JM}(q)=\frac{q}{2M}\sum_{i=1}^{A}\{\hat{g}_i j_J(qr_j)\left[\mathrm{Y}_J(\Omega_j)\times\hat{\sigma}_j\right]^{JM}+$$

$$+\frac{2\hat{e}_i}{q}(\sqrt{\frac{J+1}{2J+1}}j_{J-1}(qr_j)[Y_{J-1}(\Omega_j)\times\hat{\nabla}_j]^{JM}-$$

$$-\sqrt{\frac{J}{2J+1}}j_{J+1}(qr_j)\left[\mathrm{Y}_{J+1}(\Omega_i)\times\hat{\nabla}_i\right]^{JM})\}$$

$$\hat{T}^{mag}_{JM}(q)=\frac{iq}{2M}\sum_{i=1}^{A}\{\hat{g}_j(\sqrt{\frac{J+1}{2J+1}}j_{J-1}(qr_i)\left[\mathrm{Y}_{J-1}(\Omega_i)\times\hat{\sigma}_j\right]^{JM}-$$

$$-\sqrt{\frac{J}{2J+1}}j_{J+1}(qr_j)\left[\mathrm{Y}_{J+1}(\Omega_i)\times\hat{\sigma}_j\right]^{JM})-\qquad,(8)$$

$$-\frac{2\hat{e}_i}{q}\left(j_J(qr_j)\left[\mathrm{Y}_J(\Omega_i)\times\hat{\nabla}_j\right]^{JM}\right)\}$$

where $\hat{e}=\frac{1}{2}+\frac{\hat{\tau}_3}{2};\ \hat{g}=g_{Is}+g_{Iv}\hat{\tau}_3.$

The relative contribution of spin current component grows with momentum transfer and with multipolarity of MR. The higher miltipolarity dominate at higher transferred q. On the Fig. 1 are shown the q-dependence of summed transverse $1\ \omega$ EJ and MJ form factors calculated for ^{28}Si nucleus with HOWF. The positions of the maxima of summed form factors don't depend on nucleus.

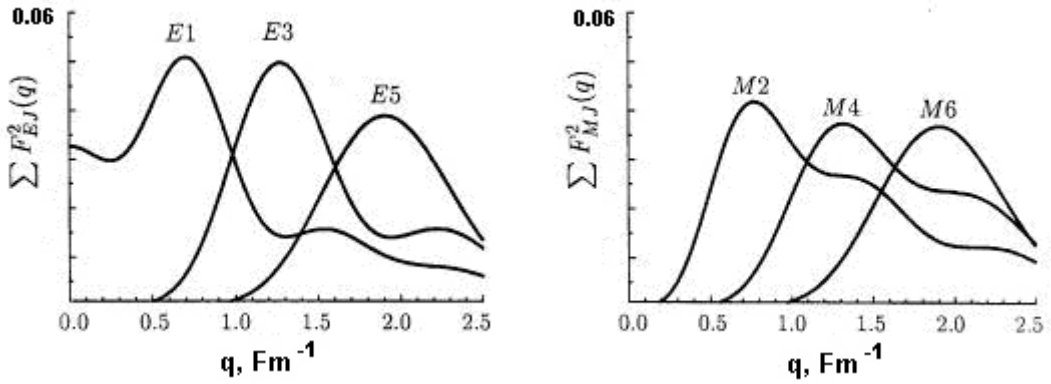

Fig.1

3. E1 resonances in photoexcitation

E1 resonances in photon absorption cross sections are determined by orbital nucleon current only. On the figures 2-7 are shown the results of PCC calculations for the form factors F^2 of dipole isovector resonances E1 at $q=E_\gamma$ together with experimental data for several sd-shell nuclei with non-filled shells. (F^2 of excited states with isospin $T=T_o$ - plain bars; $T=T_o+1$ – crossed bars).

The energy distribution of E1 form factors at photopoint in PCCSM reflects the peculiarities in spectroscopy of pick-up reaction [3] on target nucleus .

3.1. E1 in ^{22}Ne

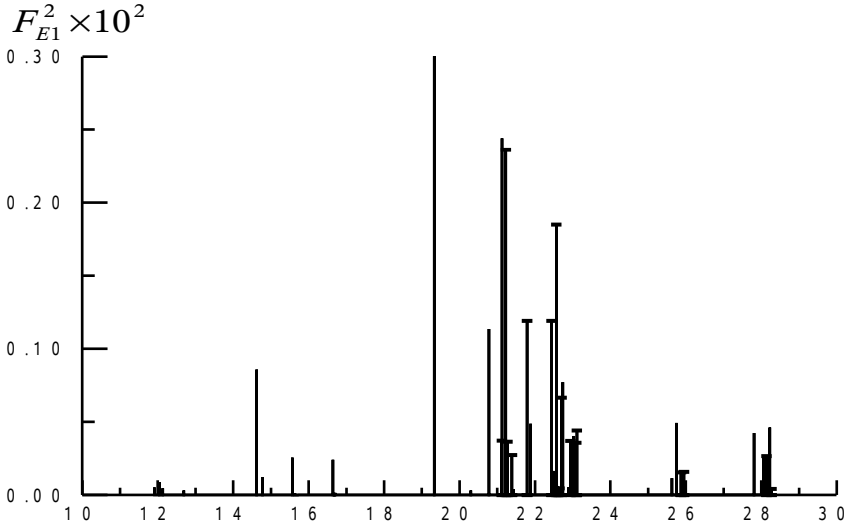

Fig. 2a

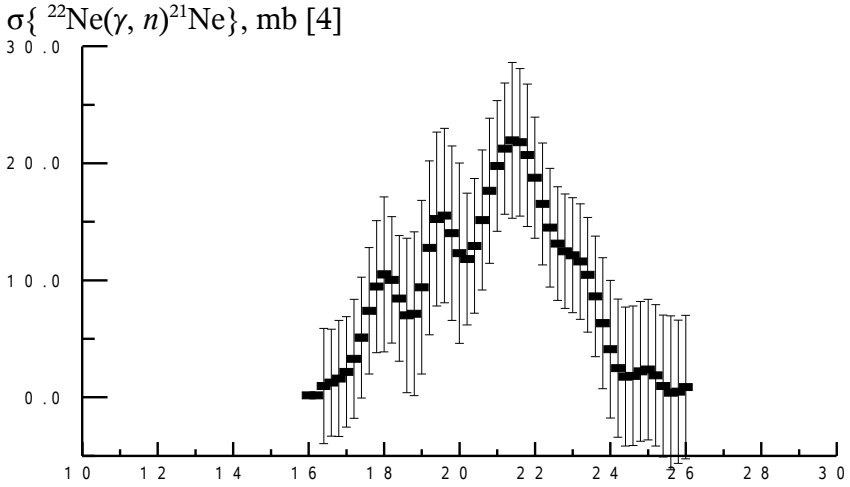

Fig. 2b

The PCC SM calculations for dipole resonance energy distribution in ^{22}Ne show that E1 strength is highly fragmented owing to isospin splitting and to wide spread of final nuclei states emerging in knockout reactions. The low energy part of Fig.2a (E< 17 MeV) is a result of transition from sd-shell.

3.2. E1 in ^{24}Mg

Among all even-even sd-shell nuclei ^{24}Mg has the largest deformation, displayed in low-lying states of rotational band. In collective description of dipole resonances in the deformed nuclei the peaks at about 20 and 25 MeV correspond to collective vibrations along and perpendicular to the axis of symmetry. PCCSM approach was based on spectroscopy factors of pick-up reactions [3]. The energy spread of states of residual nuclei with A-23, which were taken into account, is near 10 MeV.

$F_{E1}^2 \times 10^2$ $\sigma(\gamma, p)$, mb [5]

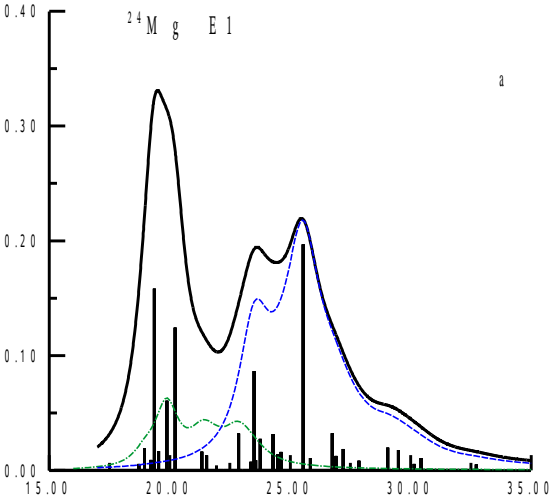

E, MeV

Fig. 3*a*

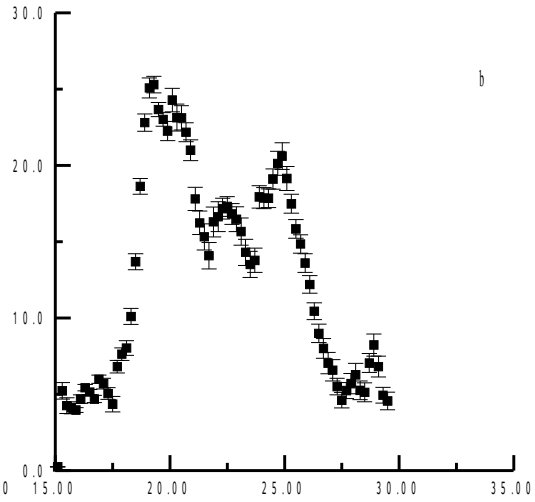

E, MeV

Fig.3*b*

The peak at 19-20 MeV is populated by transitions from $1d_{5/2}$ subshell, the 24 MeV peak is due to the transitions from 1p shell. The intermediate maximum constructed by transitions from both sd and 1p shells, with considerable contributions of configurations built on 2s and $1d_{3/2}$ hole states.

3.3. E1 in ^{26}Mg

$F_{E1}^2 \times 10^2$ $\sigma(\gamma, n)$, mb; [6]

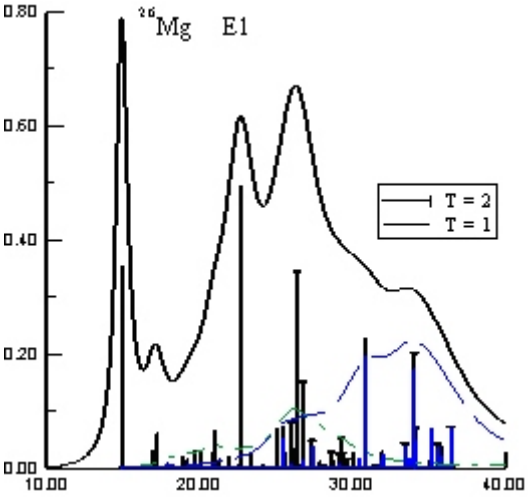

E, MeV

Fig.4*a*

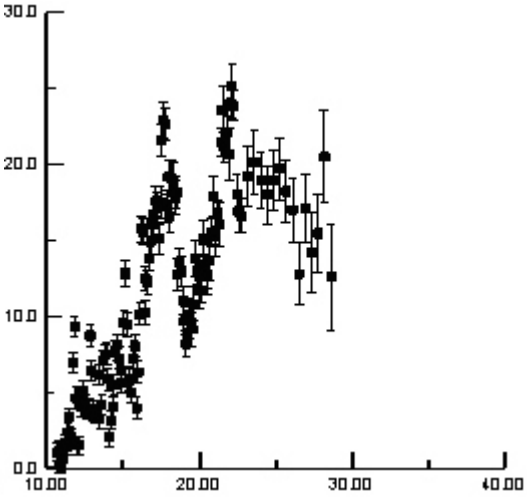

E, MeV

Fig.4*b*

The dipole resonance in ^{26}Mg nucleus has two isospin branches (T=1 – plain bars on the fig.4a and T=2 – crossed bars). The upper part of E1 energy distribution is enhanced by transitions from 1p shell with main peaks at ~31 and 35 MeV. The group of maxima at about 25 MeV contains configurations built on 2s and $1d_{3/2}$ subshells states; (γ, n) reactions in this region should populate not only $5/2^+$ but as well $1/2^+$ and $3/2^+$ states of ^{25}Mg.

3.6. E1 in S-32

$F_{E1}^2 \times 10^2$

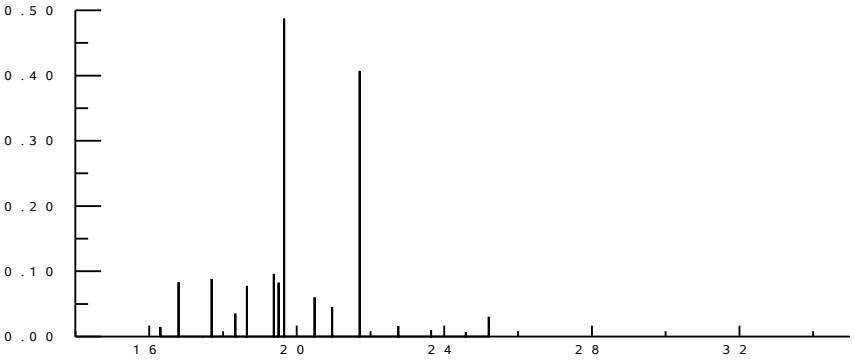

Fig.5a

$\sigma\{^{32}S(\gamma,n_{tot})\}$, mb [7]

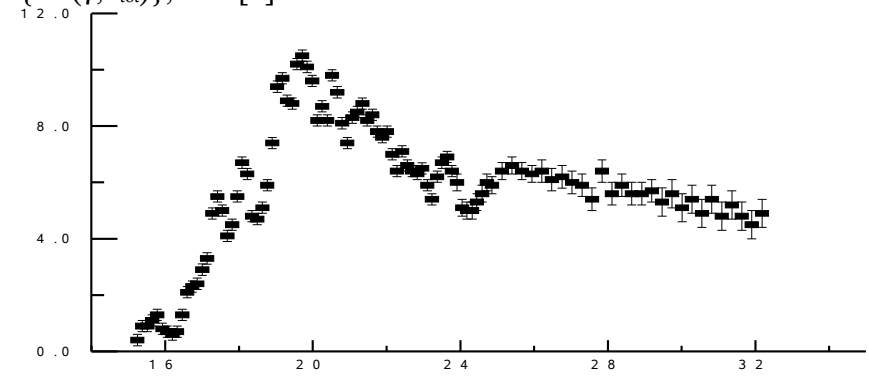

Fig.5b

E, MeV

3.6. E1 in S-34

$F_{E1}^2 \times 10^2$

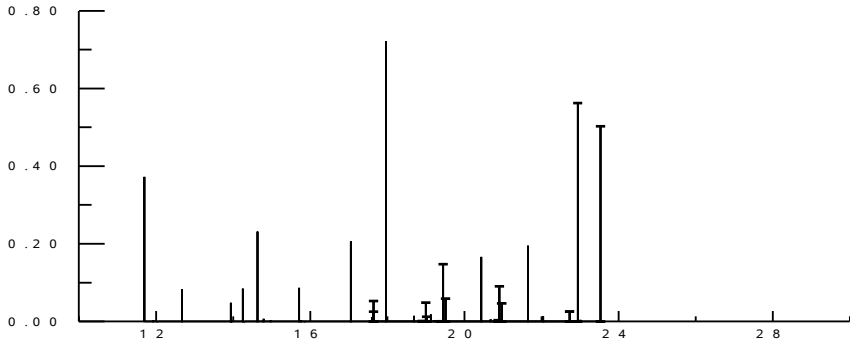

Fig.6a

$\sigma\{^{34}S(\gamma,abs)\}$, mb [8]

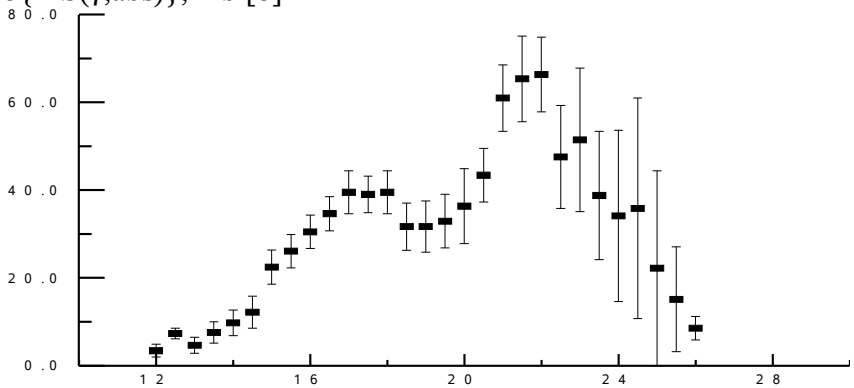

Fig.6b

E, MeV

The comparison of E1 strengths fragmentation in ^{32}S and ^{34}S reveals the influence of isospin splitting and the final nuclei energy spreading on the structure of dipole resonance.

4. M2 in sd-shell nuclei

On the Fig 7 are shown the results of PCC SM calculations for M2 form factors in ^{32}S at momentum transfer q=0.6 Fm^{-1} with comparison with the data of S-DALINAC experiment [10] performed up to energy excitation E=14 MeV. The renormalized value of g-factor was used. The spreading of the hole among 12 states of ^{31}S reveals in fragmentation of M2 strength.

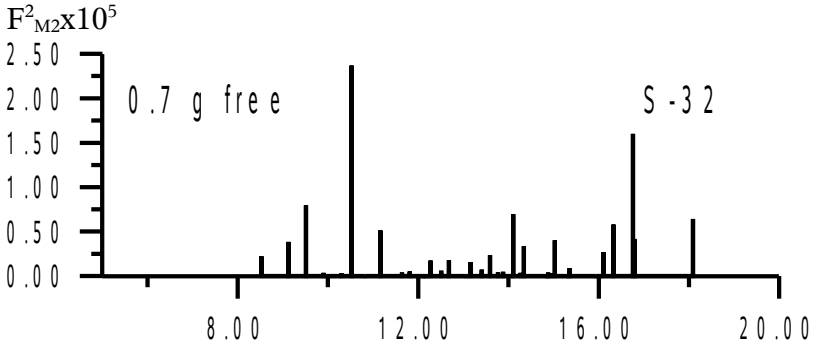

Fig.7a

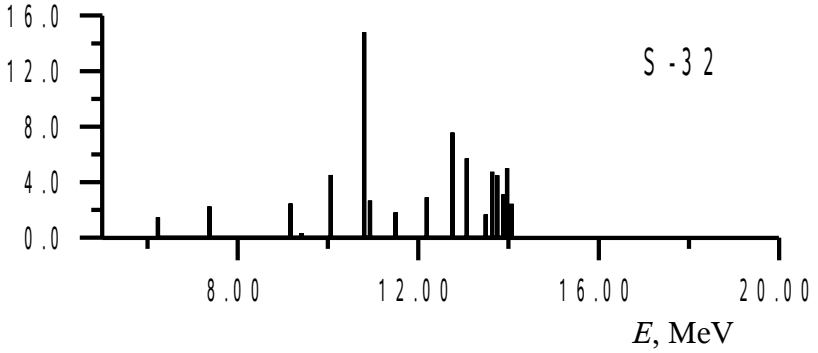

Fig.7b

In the excitation of magnetic resonances main role belongs to spin-multipole operators. For M2 resonances there are spin-dipole and spin-octupole operators in (8); the first one dominates at approximately 0<q<1Fm^{-1}, the second one at q>1Fm^{-1}. The role of orbital current contribution into matrix elements of M2 transitions was estimated for M2 form factor $F_{M2}\times10^3$ (Fig.8) taking into account the effects of interference of spin and orbital parts of M2 operator ($g=0.7g_{free}$). It is clear that the orbital current plays a very significant role in M2 excitation (the similar results were obtained for orbital current contribution into M2 resonances in ^{28}Si and ^{24}Mg). This conclusion of shell model approach confirms the results of [11] where direct evidence for orbital magnetic quadrupole twist mode in nuclei was obtained.

Contributions of spin and orbital currents into matrix elements of M2.

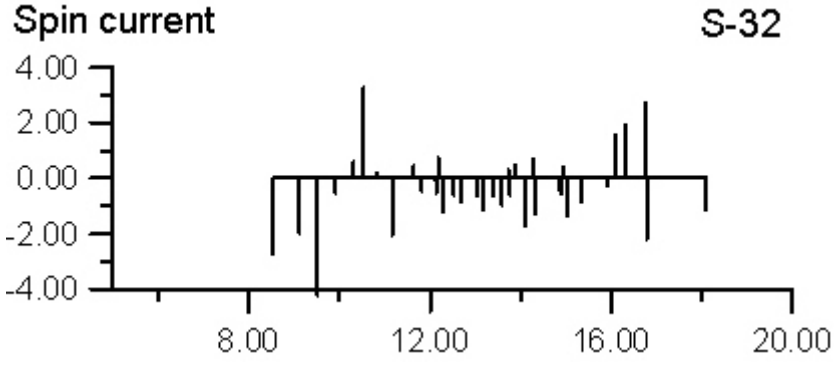

Fig 8a.

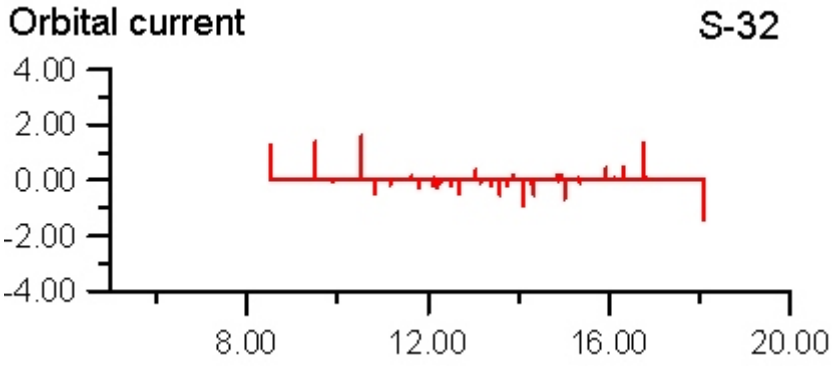

Fig 8b.

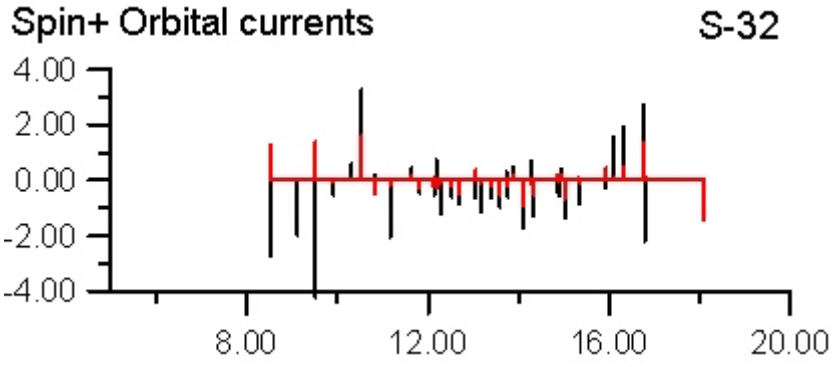

Fig 8c.

In the Fig.9 is shown the energy distribution for reduced probability B(M2) in ^{24}Mg. The fragmentation of M2 strength reflect the configurational splitting of resonance: the peaks in the 10 -16 MeV region of nuclear excitation correspond to transitions from sd-shell, the resonances at E>16 MeV are almost completely due to transitions from 1p shell. Unfortunately the S-DALINAC experiment for this nucleus was performed in the narrow range 11<E<13.4 MeV only.

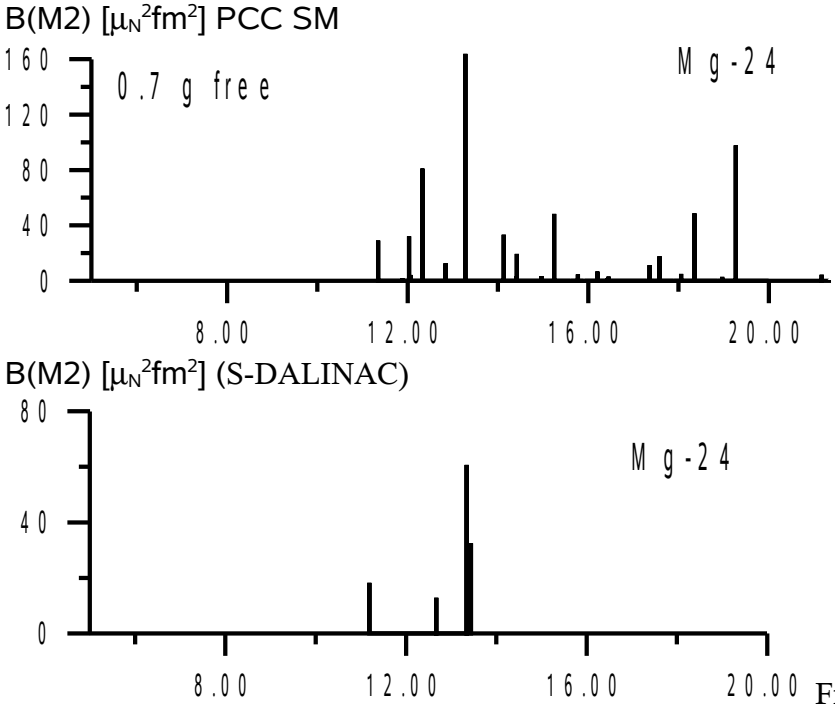

Fig 9.

4. M6 in sd-shell nuclei

The $1\hbar\omega$ resonances with maximal spin of magnetic electroexcitation reveal the influence of the hole distribution on MR fragmentation most obviously. The "doorway" states of M6 in sd-shell correspond to the transition $1d_{5/2} \rightarrow 1f_{7/2}$ only.

$F^2_{M6} \times 10^2$ $F^2_{M6} \times 10^2$

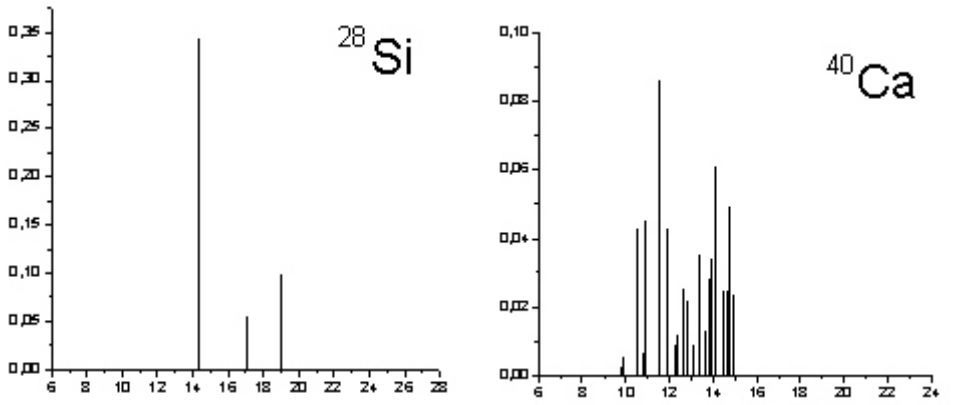

E,MeV E,MeV Fig.10

The role of hole spreading manifests in the fragmentation of 6^- T=1 states in ^{28}Si and ^{40}Ca (fig.10) according to PCCSM at q=1.8 Fm^{-1}. The M6 in ^{28}Si was the first of explored MR with maximal spin value. In (e,e') reaction on ^{40}Ca M6 was not detected. It is a result of very wide scattering of $5/2^+$ hole on 23 states in A=39 nuclei in a energy range from 2.8 up to 9.5 MeV and the following fragmentation of 6^- T=1 strength in ^{40}Ca nucleus.

The results of PCC calculations for M6 excited states in ^{26}Mg at momentum transfer q=1.8 Fm^{-1} are shown in the Fig.11 together with experimental data. (Plain bars represent T=1, crossed bars - T=2 states)

$F^2_{M6} \times 10^2$;PCC SM $F^2_{M6\,\mathrm{exp}} \times 10^3$; Exp. [12]

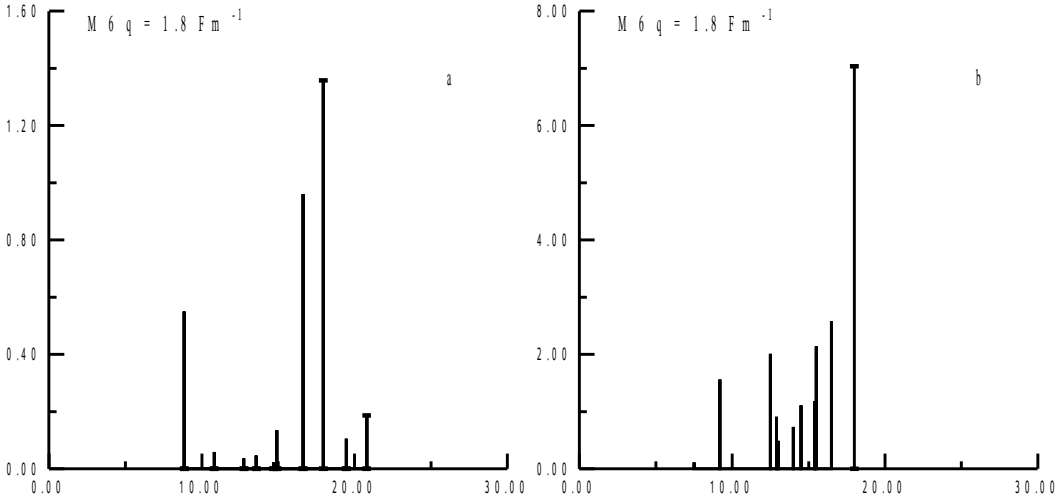

E, MeV *E*, MeV

Fig.11

.

SUMMARY

- The deviation of (A) nucleus from closed shells or subshells reveals in a wide range of energy distribution for ”hole” among the (A-1) nuclei states. In the PCC version of SM these distributions are taken into account in the microscopic description of multipole resonances.
- The energy spread of final nuclei states is the main origin of the multipole resonances fragmentation in open shell nuclei. Comparison of PCC SM results with experimental data on MR confirms the validity of this approach for a range of momentum transfer from “photopoint” up to $q \approx 2$ Fm^{-1}.
- The assumption that some very valuable information on MR in excited deformed nucleus is embedded in direct reactions data proved to be right.

REFERENCES

1. N.G.Goncharova, N.P.Yudin, Phys. Lett.**B29** (1969) 272.
2. S. Raman *et al*, Atomic Data & Nucl.Data Tables **78** (2001) 1.
3. P.M.Endt, Nucl. Phys. **A521** (1990) 1.
4. V.V.Varlamov, M.E.Stepanov, BRAS Physics **64** (2000) №3.
5. B.S. Ishkhanov *et al*, Nucl. Phys. **A186** (1972) 438.
6. S.C. Fultz, R.A. Alvarez, B.L. Berman *et al*, Phys.Rev. C **4** (1971) 149.
7. S.C. Fultz, J.T. Caldwell, B.L. Berman *et al*, Phys.Rev. **143** (1966) 790.
8. A.Veyssiere, H.Beil *et al*, Nucl. Phys. **A227** (1974) 513.
9. J. Vernotte *et al* , Nucl.Phys.A**655**(1999)415
10. F. Hoffmann, Diplomarbeit, IKP TUD (1997).
11. B. Reitz *et al,* Phys.Lett.B **532**(2002)179.
12. B.L. Clausen, R.J. Peterson, R.A. Lindgren, Phys. Rev. **C38** (1988) 589.